Nuclear Magnetic Resonance Volumetric Antenna

Achraf Waguaf, Ludivine Fadel, Valérie Vigneras, François Demontoux, Abdoulaye Fall, Hakim Takhedmit, Marjorie Grzeskowiak

Nuclear Magnetic Resonance volumetric antenna

Achraf Waguaf[1], Ludivine Fadel[2], Valérie Vigneras[2], François Demontoux[2], Abdoulaye Fall[3], Hakim Takhedmit[4], Marjorie Grzeskowiak[4]

[1] Electronic departement, ENSEIRB-MATMECA, Talence, France, achraf.waguaf@enseirb-matmeca.fr
[2] Universite de Bordeaux, Laboratoire IMS, UMR-5218, Talence, France, ludivine.fadel@ims-bordeaux.fr
[3] Laboratoire Navier (UMR 8205 CNRS, IFSTTAR, Ecole des Ponts ParisTech), Université Paris Est, Champs-sur-Marne, France
[4]Universite de Paris-Est Marne-la-Valle ESYCOM (EA 2552), UPEMLV, ESIEE-Paris, CNAM F-77454, Marne-la-Vallee, France, marjorie.grzeskowiak@univ-mlv.fr

***Abstract*—The paper proposes NMR antennas. The idea is to realize antenna dedicated to the study of unsaturated granular material. The aim is to design volumetric antenna whose small size allows increasing the measurement sensibility. The objectives are twofold: enhance the H-field homogeneity and the Signal-to-Noise Ratio.**

Index Terms—coil, magnetic field homogeneity calculation, magnetic field measurement, nuclear magnetic resonance (NMR) imaging

I. CONTEXT

How does liquid expand in wet granular material under shear? We know from everyday experience that mixing powders and liquid is a challenging task. The main reason is the internal cohesion due to capillary forces arising from liquid bridges between the grains [1-6]. Such flows are found in pharmaceutical production, the chemical industry, the food and agricultural industries, energy production and the environment. Many unsolved problems remain, however. In order to be able to solve problems, granular flows need to be understood so that their behavior can be controlled and predicted. While dry granular materials and fully saturated grain-fluid mixtures are quite extensively studied [7-9], unsaturated granular assemblies are less known. Unsaturated granular materials are composed of an assembly of grains whose pore space is partially filled by a liquid (water, oil…) and a gas. The general purpose of the project is to determine the microstructure of unsaturated granular materials in different flow regimes and liquid contents, and possibly to use this information as a starting point for the determination of macroscopic constitutive rheological laws.

The first part of this project is the development of specific tools to study and model the behavior of such materials. Magnetic Resonance Imaging (MRI) experiments are designed in order to access local information on grains and liquid content, and couple mechanical measurements with microstructural information by direct measurements of velocities, solid and liquid fractions in a annular shear device, through either 3D or '2D in a slice' imaging (Fig.1.b). Indeed, specific challenges however arise in the present project due to very low fluid volume fractions. As far as measurements of fluid velocities are concerned, some of our latest progress in methodology have provided signal to noise ratio as high as 200 in 2D slices at 5% fluid content, a result which now promises successful measurements down to 1% liquid content. The shear device is inserted into a magnetostatic uniform B_0 field and submitted to B_1^+ field emission from a radiofrequency (RF) probe, this RF field is normal to the magnetostatic one (Fig.1.a). This phase is called "absorption phase", when the system of nuclear spin is excited and has absorbed energy. During the relaxation phase, i.e. when the RF emission is stopped, the system of nuclear spins restituted energy by precession movement at nuclear magnetic resonance. In this case, RF probe measured B_1^- field in induced RF coil: the characteristics of the unsaturated granular material can be determined.

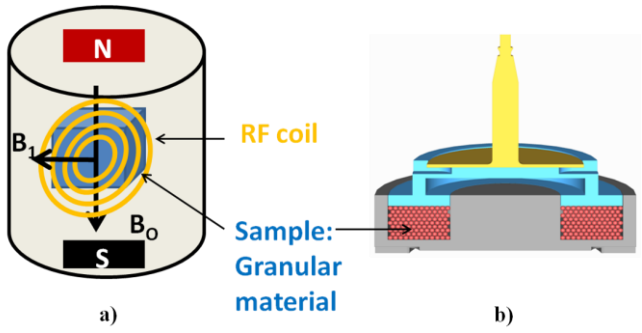

Fig.1. a) NMR setup measurement b) Cross section of the annular plane shear flow.

RF coil is designed to both optimize the SNR and H-field homogeneity [10], which represents a compromise between the reduction of length of copper tape and the complexity enhancement of the structure. RF coils can be surface coils, such as planar loops, or volumetric coils, such as solenoid coil [11-19]. The surface coils [11] provide a higher SNR, but with low homogeneity, while volumetric coils provide a homogeneous magnetic field throughout the ROI (Region Of Interest) [12]. Saddle-coil, composed of both complementary coil, wrapped around a cylindrical shape is studied in [11], versus distance between the complementary coils. Birdcage is the classical coil in NMR, with a good homogeneity but a poor SNR [10]. In [13], curved surface RF coil resonator is optimized to increase SNR throughout the ROI in keeping constant the homogeneity. Uses of

parasitic scatterers [14], of partially orthogonal resonators [15] or of high-permittivity material attachment [16] can increase the homogeneity.

II. PROBLEM STATEMENT

If the existing NMR hardware and the methodology are convenient for samples with saturation larger than 10%, lower saturations, together with the small volume of the plate-cup shear cell, will require the fabrication of local radio frequency coils integrated in the shear devices to improve the sensitivity.

The current NMR system antenna is a bird-cage structure, composed of 16 copper wires (2 cm thick and 20 cm height) placed periodically around a circle of 20 cm in diameter. This system provides a RF magnetic field perpendicular to the longitudinal axis of the main magnet. The capacitor tuning for each wire increases the uniformity of the current density along the wire and produces a 50µT dynamic magnetic field with homogeneity of 1%. However, for fluid small volumes of interest, low signal to noise ratio (SNR) is obtained. A high SNR is needed (a gain of 10 is attended) and the RF coil must be able to collect the signal emitted by the nuclei with better sensitivity throughout the volume of interest. Therefore, the coil, which produces the RF magnetic field and detects the emitted signal, must be placed around the sample during the experiment. The orientation of the RF field is not necessarily perpendicular to the magnet field, but the greater is the perpendicular component of the RF magnetic field, the best is the SNR. Furthermore, a compromise appears with the homogeneity and the SNR: the B1 field homogeneity depends on the coil complexity, versus the line width, the line shape, the coil shape, the number of turns while high SNR involves thickness and lossless lines.

The aim of this work is to introduce a coil that produces an important perpendicular component of the RF magnetic field with spatial homogeneity of 10%. The coil loop parameters can be designed by numerical methods for solving electromagnetic problems: the commercial software HFSS (High Frequency Structure Simulator), using the FEM technique, is used in both circuit parameters and magnetic field prediction, to take into account the interactions between the coil and the sample in the volume of interest. The induced current density on the conductor, by skin depth, and the modelling of the coupling between the coils and the experimental set-up (dielectric load with high conductivity, like a body phantom for instance), have to be studied in the surface and volume of the coil, for the prediction on the magnetic field homogeneity. This software can include lumped elements like the capacitor associated to the coil to realize a RLC resonant circuit, or a matching circuit to match the coil to 50 Ω source impedance.

In order to compare the different proposed antenna structures, characteristics for NMR antenna are presented, such as homogeneity and normalized SNR computed versus the highest SNR of studied structures. Then, each NMR antenna is presented with H-field cartography in transverse plane. The best antenna structure, in term of homogeneity and normalized SNR is realised.

III. MULTILOOP ANTENNA STRUCTURES

A. $\Delta B/B$, SNR and FoM

The characteristics of the coil, such as homogeneity and Signal-to-Noise Ratio are carried out under HFSS. A Figure-of-Merit (FoM), in order to evaluate the attained goals, is defined as the ratio in dB unity between the homogeneity (% unity) and the normalized SNR. The objective is to minimize the FoM.

The homogeneity is calculated within a sphere, called ROI. The homogeneity ΔB (%) of the magnetic field is determined in our case by:

$$\Delta B = \frac{B_{max}-B_{min}}{B} \quad (1)$$

where B_{max} is the maximum magnetic induction inside the sphere, B_{min} is the minimum magnetic induction inside the sphere and B indicates the average magnetic induction in the sphere. Other formulas to calculate the homogeneity depend on the B field in one point and B field in the center of the ROI [18]-[19]. While the formula in [18]-[19] allows to draw SNR mapping, we prefer using formula that gives an average SNR in ROI.

The Signal-to-Noise-Ratio is calculated in (2) from induced B_1^- field and from the noise matrices (Ψ), where E_{km} is the local electric field of voxel k from channel m, σ_k is the local conductivity of voxel k, Δx, Δy and Δz are the voxel size in x, y, and z directions [22]. During the relaxation phase, B_1^- field can be extracted by the FEM simulation by equation (3) and noise matrices by equation (4). In the case of IRM (Imaging Resonance Magnetic), SNR calculus takes into account the absorbed power by the body [23].

$$SNR = \sqrt{B_1^{-H} * \psi^{-1} * B_1^-} \quad (2)$$

$$B_1^- = \frac{(B_x - jB_y)^*}{2} \quad (3)$$

$$\psi_{mn} = \Delta x \Delta y \Delta z \times \sum_k \sigma_k (E_{km} E_{kn}^*) \ (m,n = 1,2,\dots,8) \quad (4)$$

With $\Delta x = 2mm,\ \Delta y = 2\ mm,\ \Delta z = 2\ mm$

B. Simulated antenna structures

Each coil on Fig.2 is designed with HFSS.

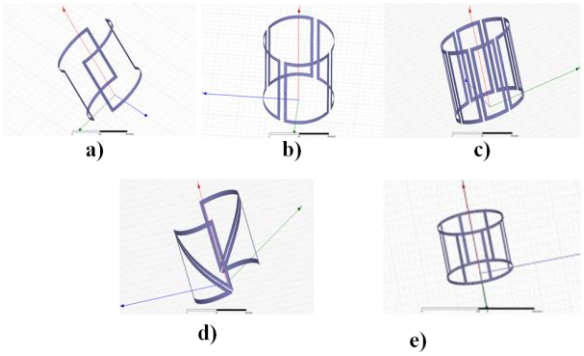

Fig.2. Structures of antennas a) saddle-coil or 2-loops coil,

b) birdcage, c) 8-loop coil, d) Z-loop coil, e) 4-loop coil
The cylindrical shape on which the coil is wrapped has a radius of 12 cm and height of 12 cm. Each metalized part is composed of 35µm thickness copper. The simulation is done with sinusoidal signal of 21.365 MHz, i.e. the Larmor frequency of the 0.5 Tesla NRM system for hydrogen atom. Each sub-loop is fed by 50Ω lumped port with 1W power, i.e. 2,4, 8, 4 and 24 ports for respectively saddle-coil, 4-loops coil, 8-loop coil, Z-loop coil and birdcage.

C. *H-field cartography and inhomogeneity versus sphrere radius*

For each antenna structure, magnitude H-field cartography is reported in the transverse plane in the center of the cylindrical shape. The magnitude H-field scale is the same in order to compare the antenna structure. The H-field is greater near the wire for the wrapped loops around the cylindrical shape and for the birdcage.

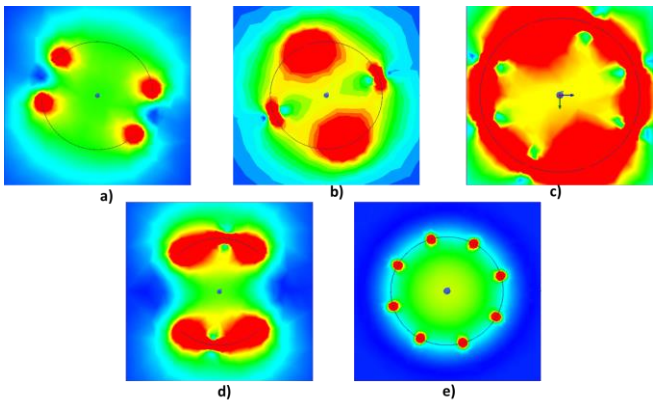

Fig.2. Magnitude H-field display of antennas in transverse plane a) saddle-coil or 2-loops coil, b) 4-loops coil, c) 8-loop coil, d) Z-loop coil, e) birdcage

The inhomogeneity of each antenna is reported on Fig. 3 versus the radius of ROI. Bird-cage and saddle-coil permit to obtain the best homogeneity whatever ROI radius.

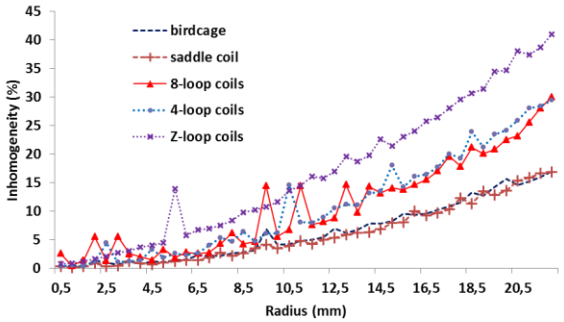

Fig.3. Inhomogeneity of each structure versus ROI radius

To realize a quantitative study, the homogeneity, normalized SNR and FoM are reported for each antenna structure inside a ROI of 7 mm radius: this radius value corresponds to homogeneity less than 10%, as expected in the specifications.

D. *Comparison with FoM*

As described in [23], and as seen in Table 1, the more complex structure of volumetric antenna is needed for the greater homogeneity, but the SNR will drop off. In addition, a small size of volumetric antenna is also required to allow enough measurement sensibility for unsaturated granular material: the diameter is multiplied by 3 and divided by 5, that corresponds to the transformation from the current RF antenna (birdcage of 20 cm diameter) to the simulated ones (12 cm diameter). Long length of antenna wire results in SNR decrease and reduced imaging results. As expected, birdcage presents the best homogeneity while the normalized SNR is weak. It seems interesting to realize the structure with the best FoM, i.e. the saddle-coil.

Table 1. Comparison of homogeneity, normalized signal-to-noise ratio and Figure of Merit for simulated antennas

Type of antenna	$\frac{\Delta B}{B}$ (%)	Normalized SNR	FoM (dB)
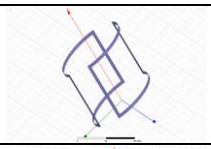	2.7	0.985	0.43
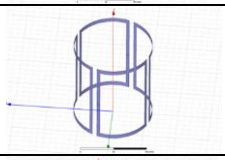	6.29	0.94	0.82
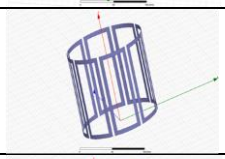	6.76	1	0.83
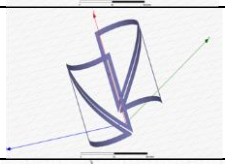	3.7	0.77	0.68
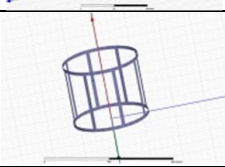	2.02	0.0006	3.52

After the realization of the RF antenna, H-field cartography has to be reported experimentally with a probe to check the homogeneity for the saddle-coil that presents the minimum FoM in ROI.

IV. STRUCTURES REALISATION AND MEASUREMENT

The coil was fabricated by stacking copper tapes on the surface of plexiglass tube (Fig.4). In a first step, in free space, the RF coil input impedance will be measured with

HP 4194A RLC meter: the objective is to match each coil on 50Ω cable with capacitors [23].

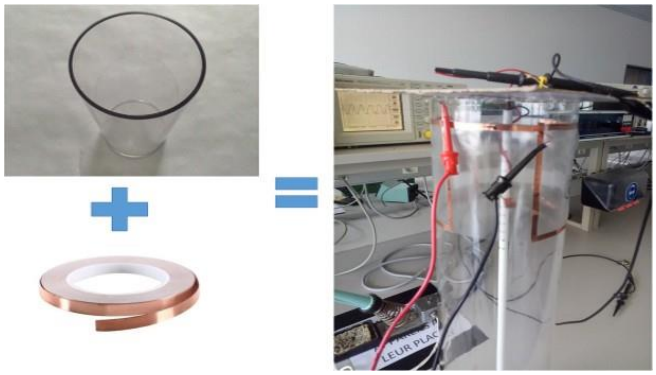

Fig.4. Fabricated saddle coil

The H-field was measuring using a homemade probe. The probe consists of 5-turn wire around a 10 mm diameter plexiglass tube (Fig.5). On figure 5, the saddle-coil and the homemade probe present respectively inductance of 0.7µH and 0.14µH.

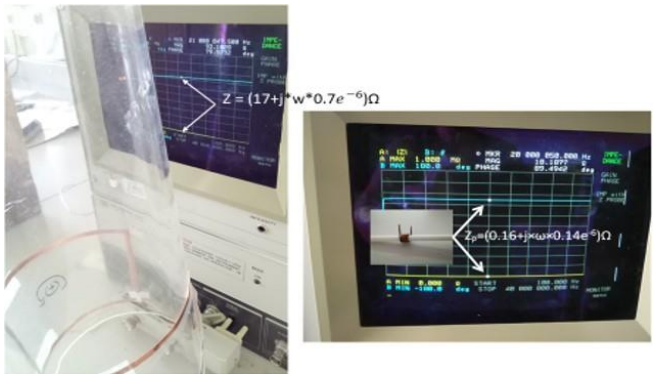

Fig.5. Impedance of sadde coil (left side) and H-field probe (right side) at 20MHz with HP 4194A RLC meter

The magnetic field generated by the RF antenna is obtained using an Agilent 33250A Signal Generator working at 20 MHz. The induced voltage on the probe is for the component normal to the antenna surface in order to best approximate the voltage measured by the probe. The induced voltage is measured with Tektronix TDS 220 oscilloscope. The cylindrical wire probe was placed firstly at the (0,0) center of the volumetric antenna and then moved in a (x0y) plane with an spatial grid as seen on Fig. 6 inside the antenna.

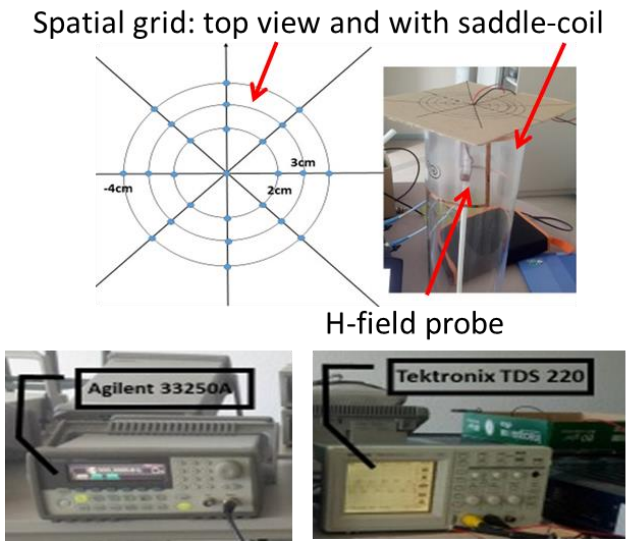

Fig.6. Bench setup (spatial grid, saddle-coil, homemade probe, generator and oscilloscope)

The induced voltage is fluctuated due to measurement disturbance and no measured accuracy result is obtained. We suppose this fluctuation comes from leakage current. We have to use ferrites to limit the influence of leakage current in the cable that connects the H-field probe to the oscilloscope [25]. Another possibility to obtain the magnetic field homogeneity by indirect measurement is to connect directly the coil into a magneto static uniform B_0 field.

V. Conclusion

Several RF coils are compared in terms of homogeneity and SNR in free-space without unsaturated granular material, with electromagnetic software; a FoM that takes into account the homogeneity and the normalized SNR is defined in order to select the best structure that is fabricated. We perform the size reduction of RF antenna by a factor 3/5 to increase the sensibility and chose a compromise between the homogeneity and the normalized SNR.

In future works, in order to prevent common mode currents that disrupt the measure of induced voltage of the probe; ferrite would be attached on the cable to report H-field cartography. The coil without load and into a magneto static uniform B_0 field could predict the magnetic field homogeneity. The coils in presence of "calibrated" dielectric loads and into a magneto static uniform B_0 field will be tested to observe the impact of the environment on the input impedance of the coils, and on the link performance between them.

Acknowledgment

This work was supported by the National Agency of Research and within the project JCJC RheoGranosat (Grant No. ANR-16-CE08-0005-01).

References

[1] T. Mikami, H. Kamiya, and M. Horio, Chem. Eng. Sci. 53, 1927 (1998).

[2] J. N. Israelachvili, Intermolecular and Surface Forces (Academic, London, 1991), 2nd ed.

[3] D. J. Hornbaker, R. Albert, I. Albert, A.-L. Barabasi, and P. Schiffer, Nature (London) 387, 765 (1997).

[4] T. C. Halsey and A. J. Levine, Phys. Rev. Lett. 80, 3141 (1998).

[5] L. Bocquet, E. Charlaix, S. Ciliberto, and J. Crassous, Nature (London) 396, 735 (1998).

[6] N. Fraysse, H. Thomé, and L. Petit, Eur. Phys. J. B11, 615 (1999).

[7] B. Andreotti, Y. Forterre and O. Pouliquen, Granular Media: Between Fluid and Solid, Cambridge University Press, 2013.

[8] GDR Midi. On dense granular flows. Euro. Phys. Journ. E., 14:341-365, (2004).

[9] A. Fall, G. Ovarlez, D. Hautemayou, C. Mézière, J.-N. Roux, F. Chevoir, Dry granular flows : Rheological measurements of the μ (I) - rheology, J. Rheol. 59 (2015), 1065–1080.

[10] J. Mispelter & al., "Nmr Probeheads for Biophysical And Biomedical Experiments: Theoretical Principles And Practical Guidelines", (2006)

[11] F. Bonetto, E. Anoardo, M. Polell, Saddle Coils for Uniform Static Magnetic Field Generation in NMR Experiments, Concepts in Magnetic Resonance Part B (Magnetic Resonance Engineering), Vol. 29B(1) 9–19 (2006)

[12] J. Schöpfer, S. Biber, M. Vossiek, Comparison of local transmit antennas for extremity imaging in MRI, GeMiC 2015 • March 16–18, Nürnberg, Germany, pp.115- 118 (2015)

[13] H. Yoo, Combined RF coils for brain imaging at 7 T with receive and transmit resonators, Electronics Letters, Vol. 52 No. 20 pp. 1662–1663 (2016)

[14] J. D. Sánchez-Heredia, J. Avendal, A. Bibic, B. Kiong Lau, Radiative MRI Coil Design Using Parasitic Scatterers: MRI Yagi, Transactions on Antennas and Propagation, Vol. 66 No. 3 , pp.1570-1575, (2018)

[15] J. Chacon-Caldera, M. Malzacher, L. R. Schad, Partially orthogonal resonators for magnetic resonance imaging, Scientific Reports, DOI: 10.1038/srep42347 (2017)

[16] J.-H. Seo, S.-D. Han and K.-N. Kim, Improvements in magnetic field intensity and uniformity for small-animal MRI through a high-permittivity material attachment, Electronics Letters, Vol. 52 No. 11 pp. 898–900 (2016)

[17] A. Kordzadeh, N. De Zanche, Control of Mutual Coupling in High-Field MRI Transmit Arrays in the Presence of High-Permittivity Liners, IEEE Transactions on Microwave Theory and Techniques, , Vol. 65, No. 9, pp. 3485-3491, (2017)

[18] Z. Chen, K. Solbach, D. Erni, A. Rennings, Field Distribution and Coupling Investigation of an Eight-Channel RF Coil Consisting of Different Dipole Coil Elements for 7 T MRI, IEEE Transactions on Biomedical engineering, Vol. 64, No. 6, pp. 1297-1304, (2017)

[19] A. Nikulin, S. Glybovski, I. Melchakova, P. Belov, S. Enoch, R. Abdeddaim, A Dual-Frequency MRI Coil for Small Animal Imaging at 7 Tesla Based on Metamaterial-InspiredWire Structures, IEEE International Congress on Advanced Electromagnetic Materials in Microwaves and Optics – Metamaterials, pp. 241-243 (2016)

[20] I. Frollo , P. Andris, A. Krafcík, D. Gogola, and T. Dermek, Magnetic Field Homogeneity Adjustment for Magnetic Resonance Imaging Equipment, IEEE Transactions on Magnetics, Vol. 54, No. 5 (2018)

[21] S. Karmakar Ghosh, V. Thakur, S. Roy Chowdhury, Design and simulations of low cost and low magnetic field MRI system, IEEE International Conference on Sensing Technology (ICST), (2017)

[22] X. Yan, Z. Cao, X. Zhang, Simulation verification of SNR and parallel imaging mprovements by ICE-decoupled loop array in MRI, Applied Magnetic Resonance, Vol. 47, No.4, pp. 395-403 (2016)

[23] C.Wang, G. X Shen, B1 Field, SAR, and SNR Comparisons for Birdcage, TEM, and Microstrip Coils at 7T, Journal of Magnetic Resonance Imaging Vol. 24, pp. 439-443 (2006)

[24] RFID Handbook, Wiley second edition, Klaus Finkenzeller, pp.322-325 (2003)

[25] Juan D. Sánchez-Heredia, Johan Avendal, Adnan Bibic, Buon Kiong Lau, Radiative MRI Coil Design Using Parasitic Scatterers MRI Yagi, IEEE Transactions on Antennasq and Propagation, Vol.66, N°3, pp. 1570-1575 (2018)